



## Design of a pressure sensor of 0–7 bar in fiber optic using MMI methodology



A.R. Mejía-Aranda<sup>a,1</sup>, V.I. Ruiz-Perez<sup>b,2</sup>, M.A. Basurto-Pensado<sup>a,\*</sup>, E.E. Antúnez-Cerón<sup>a,1</sup>, D.A. May-Arrijo<sup>c,3</sup>, P. LiKamWa<sup>d,4</sup>, J.J. Sanchez-Mondragon<sup>b,2</sup>

<sup>a</sup> Centro de Investigación en Ingeniería y Ciencias Aplicadas (CIICAp), Universidad Autónoma del Estado de Morelos (UAEM), Av. Universidad 1001, Col. Chamilpa, 62210 Cuernavaca, Morelos, Mexico

<sup>b</sup> Departamento de Óptica, Instituto Nacional de Astrofísica Óptica y Electrónica, Luis Enrique Erro No. 1, A.P. 51 y 216, C.P. 72000, Tonantzintla, Puebla, Mexico

<sup>c</sup> Universidad Autónoma de Tamaulipas, Matamoros 8 y 9, Col. Centro, C.P. 87000, CD. Victoria, Tamaulipas, Mexico

<sup>d</sup> CREOL, The College of Optics and Photonics, University of Central Florida, 4000 Central Florida Blvd., Orlando, FL 32816, USA

### ARTICLE INFO

#### Article history:

Received 21 November 2012

Accepted 18 April 2013

#### Keywords:

FOPS  
Diaphragm  
Multimode interference  
Bending  
Alternative

### ABSTRACT

This research shows the possibility of measuring pressure in the range of 0–7 bar and the comparison against 2 commercial sensors. The technique used is based on the multimodal interference in a fiber optic singlemode–multimode–singlemode (SMS) to 1550 nm. The fiber optic is mounted on a plate of stainless steel AISI 316, where the bending of the plate will generate a curvature on the part of the multimodal fiber generating a decoupling of modes and this generates a low intensity to the output of the system.

© 2013 Elsevier GmbH. All rights reserved.

### 1. Introduction

Sensor development is a constantly evolving field, and within the most important variables for industry includes temperature, vibration and pressure.

Pressure sensors are typically based on electronic devices, but there are places where electronics cannot be easily implemented because of extreme conditions such as high temperature, high corrosive areas, or tight places with high EMI. Based on this type of problem, is that we have been studying different techniques of pressure measurement based on optical media, being in our best interest Fiber Optic Pressure Sensors (FOPS) because the non-contact optical fiber any power, generates no heat, is immune to electromagnetic interference, can transport your large distance with minimal loss and is very thin.

The literature show that the majority of fiber optical pressure sensors are fiber Bragg gratings based in [1–6], Fabry–Perot Resonators [7–10] and bending techniques such as microbending loss [11] and macrobending [12]. In this paper, the multimode interference (MMI) and the reimaging theory occurring in a singlemode–multimode–singlemode (SMS) fiber structure is used in pressure measurement applications. The operation of the sensor is based on effective refractive index variations, which are achieved when a section of MMF without cladding is covered by any appropriate gradually proportionally to the pressure equipment increments. This asymmetric distribution of cladding will result on an effective refractive index variation and the spectral response consequent changes. Under this configuration, intensity changes are obtained by tracking in a special wavelength, which are correlated to the pressure values. A linear response and high repeatability are obtained. The aim is to produce a reliable, easy to manufacture and low-cost pressure sensor. All these requirements are brilliant with our proposed sensor, because of its configuration quite simple, inexpensive intensity-based detection system and easy signal processing.

The operation of the proposed sensor is based on the effect of multimodal interference (MMI), which is used in the development of planar waveguides and in the last decade have been studying optical fiber singlemode–multimode–singlemode (SMS). The

\* Corresponding author. Tel.: +52 777 3297084.

E-mail address: [mbasurto@uaem.mx](mailto:mbasurto@uaem.mx) (M.A. Basurto-Pensado).

<sup>1</sup> Tel.: +52 777 3297084.

<sup>2</sup> Tel.: +52 222 2663100.

<sup>3</sup> Tel.: +52 899 9213300x8315; fax: +52 899 9213301.

<sup>4</sup> Tel.: +1 407 8236816.



Fig. 1. SMS fiber structure.

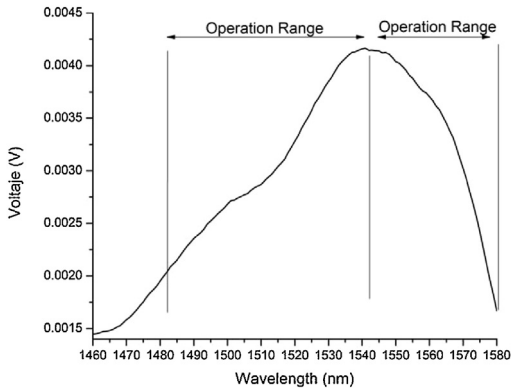


Fig. 2. Profile for SMS with  $p = 1/4$ .

fundamental principle of this development is based on the phenomenon of self-image (self-imaging), which is defined as: “the property of multimode waveguides in which an input field profile is reproduced in single or multiple images at periodic intervals along the propagation direction of the waveguide” [13].

**2. Principle of operation**

The arrangement which we will build a singlemode fiber (SMF), a multimode (MMF) and singlemode (SMF), as seen in Fig. 1, to which we will call SMS (singlemode–multimode–singlemode).

The main part of this structure is based on the distance of the MMF section, which bear the guided modes within it which will be forming single or multiple images at regular intervals along the propagation direction, due to the interference of the guided modes.

The self-image distance is given by the equation 1 is often referred to as re-image distance [14,15] and is used for determination of the length of the MMF in SMS structure.

$$L_{\text{self-image}} = p \frac{16n_{\text{core}}d}{\lambda}; \quad p = 0, 1, 2, 3, \dots \quad (1)$$

The distance  $L_{\text{self-image}}$  is a function of the wavelength  $\lambda$  (the light source to be operated), the NOCORE refractive index and radius of the core of the MMF fiber, the parameter  $p$  denotes the number of self-images, but also to a self image can be divided into periodic intervals of 4 ( $p = 1/4, 1/2, 1/3$  and 1). The difference between a profile with  $p = 1$  and  $p = 1/4$ , is that the former have a higher amplitude but a narrow width, whereas the second will be lower and its amplitude will be wider profile, Fig. 2 shows a profile for  $p = 1/4$ .

In Fig. 2, it can be seen as the left side of the profile has a gentler slope than the right side. In our case we will work with the right side.

The MMF used in this case is a special fiber known as being non-core or core lacking a large core fiber without coating. MMF parameters used have a diameter of 125 microns and refractive index of 1.44402.

**3. Experimental setup**

The arrangement proposed for characterizing the output voltage of fiber passing through the MMI is presented in Fig. 3.

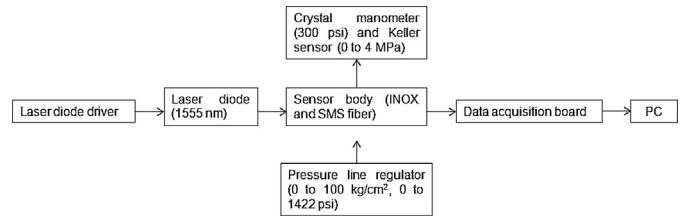


Fig. 3. Settlement proposed for data acquisition.

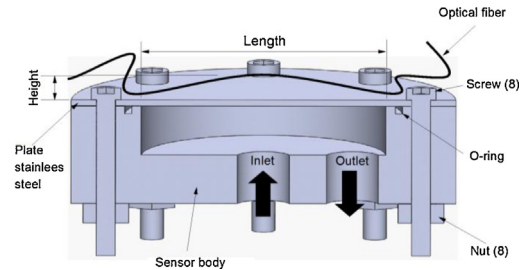


Fig. 4. Diagram sensor.

The arrangement comprises the following: (a) current driver or power controller for the laser diode, (b) diode laser (1555 nm), (c) the sensor body and a stainless steel plate is placed on the fiber where SMS, (d) data acquisition board (receiving voltage data), (e) crystal gauge 300 psi (2.07 MPa) and Keller sensor MPA of 0–4, (f) pressure regulator of the air supply line from 0 to 9.8 MPa and (g) PC.

**4. Experimental results**

Fig. 4 shows a scheme of the used sensor, the sensor body is Nylamid to avoid leakage is placed an O-ring of 4” between the mold and a 316 stainless steel plate of 1.7 mm thick, sealed by 8 screws (see Fig. 4).

On steel plate, place the uncoated fiber SMS arcing, to know what the best answer in voltage is variable height and distance fiber SMS where the arc starts, for the value of the distance is considered the start of the cavity housing the air toward the center of the sensor. Characterized the signal response taking two distances: 5 mm (Fig. 5) and 10 mm (Fig. 6) from each end.

These tests established a height and distance based on that sweep is performed to see its behavior pressures in the output voltage of the fiber. From the above figures (Figs. 5 and 6) can be observed as increases as the height of the arc of the curve, the signal voltage in the shaft widens and then decreases. The best answer that presents itself is at a height of 3 mm

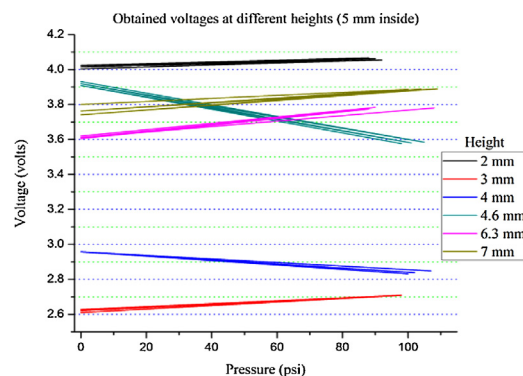
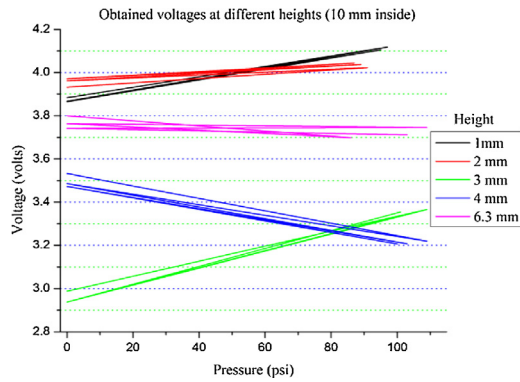
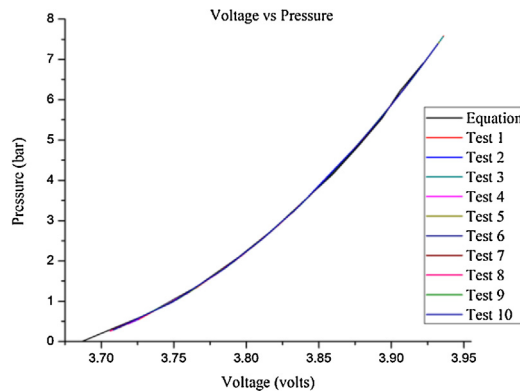


Fig. 5. Response of the fiber at different heights at a distance of 5 mm at a pressure range of 0–110 psi (0.76 MPa).



**Fig. 6.** Response of the fiber at different heights at a distance of 10 mm, in a pressure range of 0–120 psi (0.83 MPa).



**Fig. 7.** Tests to determine the behavior of signal.

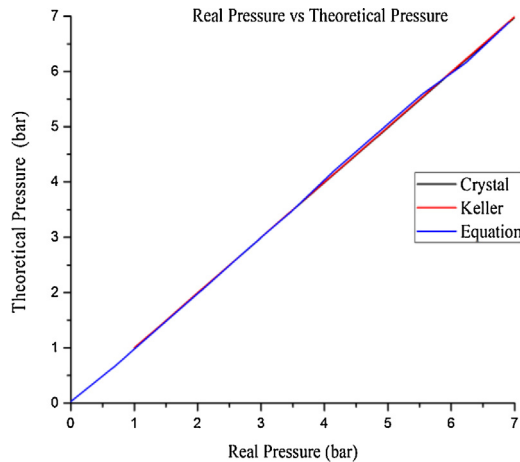


**Fig. 8.** Response of the sensors against a reference standard.

and 10 mm distance, where the voltage range of 2.93 V goes to 3.35 V, which gives us a working window of 0.42 V, and that the greater is this window we can get more resolution, since the range of 5 mm to obtain a maximum working window of 0.35 V.

Having determined the working distance and height, we proceeded to make a series of sweeps to determine the repeatability of the phenomenon and thus obtain a relationship between the

pressure measured at a reference sensor (Keller PR33) and the intensity of the signal, leading result the behavior shown in Fig. 7.

From these tests we obtained the following quadratic expression:

$$\text{Pressure} = 80.58463X^2 - 583.98169X + 1057.70841 \quad (2)$$

With a  $R^2 = 0.99965$ .

In order to compare the variation of the signal between the sensors, a test was performed between 3 sensors (SMS, Keller and Crystal PR33) against a dead weight balance as the reference, which resulted in the following graph (Fig. 8).

In this figure it can be seen that the three signals are similar but have very small differences. The three signals have the same behavior but in the range where you can see a slight difference is between 4 and 6 bar, where the response of our equation presents a percentage difference of 0.96% against the sensor and sensor Crystal Keller.

## 5. Conclusions

Using this technique it was shown that it is possible to measure the variation of pressure sensing power transmitted by the fiber. For this arrangement was established an equation with an adjustment factor ( $R^2$ ) of 0.99965. Comparison test between different measurement systems are very close, showing an error of 0.11% between them. Taking the sensor Keller (commercial sensor), the equation shows an error of 0.96% in the 4–6 bar.

## Acknowledgments

This work was supported by CONACyT, project 169197.

## References

- [1] W. Zhang, F. Li, Y. Liu, FBG pressure sensor based on the double shell cylinder with temperature compensation, *Measurement* 42 (2009) 408–411.
- [2] J. Yang, Y. Zhao, B.-J. Peng, X. Wan, Temperature-compensated high pressure FBG sensor with a bulk-modulus and self-demodulation method, *Sensor. Actuat. A* 118 (2005) 254–258.
- [3] Z. Wei, D. Song, Q. Zhao, H. Cui, High pressure sensor based on fiber Bragg grating and carbon fiber laminated composite, *IEEE Sensors J.* 8 (2008) 1615–1619.
- [4] W. Zhang, F. Li, Y. Liu, Fiber Bragg grating pressure sensor with ultrahigh sensitivity and reduced temperature sensitivity, *Opt. Eng.* 48 (2) (2009).
- [5] T. Guo, Q. Zhao, H. Zhang, C. Zhang, G. Huang, L. Xue, X. Dong, Temperature-insensitive fiber Bragg grating dynamic pressure sensing system, *Opt. Lett.* 31 (15) (2006) 2269–2271.
- [6] H.-J. Sheng, W.-F. Liu, K.-R. Lin, S.-S. Bor, M.-Y. Fu, High sensitivity temperature-independent differential pressure sensor using fiber Bragg gratings, *Opt. Exp.* 16 (20) (2008) 16013–16018.
- [7] K. Totsu, Y. Haga, M. Esashi, Ultra-miniature fiber-optic pressure sensor using white-light interferometry, *J. Micromech. Microeng.* 15 (2005) 71–79.
- [8] E. Cibula, D. Donlagic, Miniature fiber-optic pressure sensor with a polymer diaphragm, *Appl. Opt.* 44 (2005) 3264–3267.
- [9] Z. Huang, W. Peng, J. Xu, G.R. Pickrell, A. Wang, Fiber temperature sensor for high-pressure environment, *Opt. Eng.* 44 (10) (2005).
- [10] K. Alexander Sang, C. Boyd, An integrated high-pressure, pressure temperature and skin friction sensor, *Fiber Opt. Sensor. Appl.* VI 7316 (2009).
- [11] N.K. Pandey, B.C. Yadav, Embedded fibre optic microbend sensor for measurement of high pressure and crack detection, *Sensor. Actuat. A* 128 (2006) 33–36.
- [12] C. Huang, W. Wang, W. Wu, W. Ledoux, Composite optical bend loss sensor for pressure and shear measurement, *IEEE Sensors J.* 7 (2007) 1554–1565.
- [13] L.B. Soldano, E.C.M. Pennings, Optical multimode interference devices based on self-imaging: principles and applications, *J. Lightwave Technol.* 13 (1995) 615–627.
- [14] W.S. Mohammed, A. Mehta, E.G. Johnson, Wavelength tunable fibers lens based on multimode interference, *J. Lightwave Technol.* 22 (2004) 469–477.
- [15] J.E. Antonio-Lopez, A. Castillo-Guzman, D.A. May-Arrijoja, R. Selvas-Aguilar, P. LiKamWa, Tunable multimode-interference bandpass fiber filter, *Opt. Lett.* 35 (2010) 9439–9445.